uicc
global cancer control

IJC
International Journal of Cancer

Radiolabeled cetuximab: dose optimization for epidermal growth factor receptor imaging in a head-and-neck squamous cell carcinoma model

Bianca A.W. Hoeben[1], Janneke D.M. Molkenboer-Kuenen[2], Wim J.G. Oyen[2], Wenny J.M. Peeters[1], Johannes H.A.M. Kaanders[1], Johan Bussink[1] and Otto C. Boerman[2]

[1] Department of Radiation Oncology, Radboud University Nijmegen Medical Centre, Nijmegen, The Netherlands
[2] Department of Nuclear Medicine, Radboud University Nijmegen Medical Centre, Nijmegen, The Netherlands

Noninvasive imaging of the epidermal growth factor receptor (EGFR) in head-and-neck squamous cell carcinoma could be of value to select patients for EGFR-targeted therapy. We assessed dose optimization of ^{111}Indium-DTPA-cetuximab (^{111}In-cetuximab) for EGFR imaging in a head-and-neck squamous cell carcinoma xenograft model. ^{111}In-cetuximab slowly internalized into FaDu cells *in vitro*, amounting to 1.0×10^4 molecules cetuximab per cell after 24 hr (15.8% of added activity). In nude mice with subcutaneous FaDu xenograft tumors, a protein dose escalation study with ^{111}In-cetuximab showed highest specific accumulation in tumors at protein doses between 1 and 30 μg per mouse (mean tumor uptake 33.1 ± 3.1%ID/g, 3 days postinjection (p.i.)). The biodistribution of ^{111}In-cetuximab and ^{125}I-cetuximab was determined at 1, 3 and 7 days p.i. at optimal protein dose. Tumor uptake was favorable for ^{111}In-cetuximab compared to ^{125}I-cetuximab. With pixel-by-pixel analysis, good correlations were found between intratumoral distribution of ^{111}In-cetuximab as determined by autoradiography and EGFR expression in the same tumor sections as determined immunohistochemically (mean $r = 0.74 \pm 0.14$; all correlations $p < 0.0001$). Micro Single Photon Emission Computed Tomography (MicroSPECT) scans clearly visualized FaDu tumors from 1 day p.i. onward and tumor-to-background contrast increased until 7 days p.i. (tumor-to-liver ratios 0.58 ± 0.24, 3.42 ± 0.66, 8.99 ± 4.66 and 16.33 ± 11.56, at day 0, day 1, day 3 and day 7 p.i., respectively). Our study suggests that, at optimal cetuximab imaging dose, ^{111}In-cetuximab can be used for visualization of EGFR expression in head-and-neck squamous cell carcinoma using SPECT.

Key words: cetuximab, preclinical imaging, SPECT, antibody, head-and-neck cancer

Abbreviations: BSA: bovine serum albumin; Bq: becquerel; EGF: epidermal growth factor; EGFR: epidermal growth factor receptor; hr: hours; HE: Hematoxylin and Eosin; ^{125}I: ^{125}Iodine; %ID/g: percentage of injected dose per gram; ^{111}In: ^{111}Indium; IRF: immunoreactive fraction; ITC-DTPA: isothiocyanatobenzyl-diethylenetriaminepentaacetic acid; ITLC: instant thin-layer chromatography; i.v.: intravenous; mAbs: molecular antibodies; MBq: megabecquerel; MES: M 2-(*N*-morpholino)ethanesulfonic acid; min: minutes; PAD: primary antibody diluent; PBS: phosphate buffered saline; p.i.: postinjection; ROI: region of interest; RT: room temperature; s.c.: subcutaneous; SPECT: single photon emission computed tomography; T1/2 = half-life

DOI: 10.1002/ijc.25727

History: Received 23 Jul 2010; Accepted 21 Sep 2010; Online 18 Oct 2010

Correspondence to: Bianca A.W. Hoeben, Radboud University Nijmegen Medical Centre, Department of Radiation Oncology, PO Box 9101, 6500 HB Nijmegen, The Netherlands,
Tel.: +31-24-3614515, Fax: +31-24-3610792, E-mail: b.hoeben@rther.umcn.nl

Introduction

Targeted therapy is becoming an increasingly important component in the treatment of cancer. Growth factor receptors form a class of therapeutic targets regulating proliferation, differentiation and survival of malignant cells.[1] The epidermal growth factor receptor (EGFR), a receptor tyrosine kinase, is overexpressed in the majority of epithelial malignancies and plays a pivotal role in cellular proliferation, DNA repair and regulation responses to hypoxia—three major parameters determining radiation resistance.[2,3] Furthermore, EGFR overexpression is associated with advanced tumor stage and poor prognosis in several epithelial cancer types, among which head-and-neck cancer.[4,5] Treatment resistance can be counteracted by blockage of EGFR signaling with anti-EGFR antibodies such as IMC-C225 (cetuximab, Erbitux) and panitumumab (ABX-EGF, Vectibix). Cetuximab is a chimeric IgG1 monoclonal antibody (mAb) that binds to EGFR with high affinity. It competitively inhibits EGF binding to EGFR and is internalized to an extent comparable to EGF. The antibody downregulates surface EGFR expression in a dose-dependent manner and does not elicit receptor phosphorylation.[6] Cetuximab has been shown to potentiate the antitumor effect of chemotherapeutic agents.[7,8] Furthermore, addition of cetuximab to radiotherapy for locoregionally advanced head-and-neck cancer has

shown improved locoregional control and overall survival in comparison with radiotherapy alone.[9,10] However, not all patients respond to EGFR inhibition, but all patients experience toxicity induced by these therapeutics. Monitoring of biologically relevant tumor characteristics before treatment may enable selection of patients on an individual basis. Most assays are limited in that they require invasive sampling and are prone to sampling errors, therefore impeding their introduction into routine clinical practice. Noninvasive imaging with anti-EGFR antibodies could enable visualization and quantification of tumor EGFR expression, thereby aiding in the choice to commence EGFR-targeted therapy, or to assess therapeutic response to, for example, radiotherapy.[11]

Preclinical monoclonal antibody imaging studies of EGFR have been performed in various tumor models, among which head-and-neck squamous cell carcinoma cell lines, with cetuximab and other mAbs.[12–19] Results of the various studies show discrepancies as to whether the uptake of the used radiotracer accurately represents tumoral EGFR expression. Factors such as tumor vascularity and permeability and inherent pharmacodynamic properties of radiotracers play a considerable role in proper EGFR imaging. However, setup of the various preclinical studies varies, with differences for instance in methods of quantifying EGFR expression in the studied tumor models, in injected cetuximab dose, (non)residualizing properties of used radionuclides and time interval between injection of radiolabeled cetuximab and imaging. Clinical mAb (C)225 imaging studies are scarce and of a preliminary or radiodosimetric nature.[20,21]

The aim of our study was to optimize a noninvasive cetuximab-based imaging method of EGFR expression in a head-and-neck squamous cell carcinoma xenograft model. For this purpose, cetuximab was radiolabeled with ^{111}In and ^{125}I. Internalization kinetics of the radiolabeled cetuximab in FaDu tumor cells were studied *in vitro*. Specificity of radiolabeled cetuximab accumulation in the EGFR expressing tumors was determined. We investigated the effect of the antibody protein dose on tumor uptake. In addition, the pharmacodynamics of ^{111}In-cetuximab and ^{125}I-cetuximab were examined. Tumor targeting of radiolabeled cetuximab was imaged longitudinally using single photon emission computed tomography (SPECT). Tumor EGFR expression as determined immunohistochemically was compared to the intratumoral distribution of radiolabeled cetuximab by autoradiography.

Material and Methods

Radiolabeling and quality control

Radiolabeling of cetuximab. Cetuximab 5 mg/mL (Erbitux®, Merck, Darmstadt, Germany) (K_D = 0.15–0.36 nM)[22,23] was conjugated to isothiocyanatobenzyl-diethylenetriaminepentaacetic acid (ITC-DTPA, Macrocyclis, Dallas, TX) in 0.1 M $NaHCO_3$, pH 9.5, for 1 hr at room temperature (RT), using a 50-fold molar excess of ITC-DTPA. Unbound ITC-DTPA was removed by dialysis against 0.25 M ammonium acetate buffer, pH 5.5. The DTPA-cetuximab conjugate (1 mg/mL) was radiolabeled with ^{111}In (0.63 MBq/μL) (Covidien, Petten, The Netherlands), either in a 0.25 M ammonium acetate buffer, pH 5.5, for dose escalation and internalization studies, or in 0.1 M 2-(*N*-morpholino)ethanesulfonic acid (MES) buffer, pH 5.5, for microSPECT imaging and autoradiography. The scale of the radiolabeling procedure depended on the required amount of radiolabeled antibody in each experiment. Labeling continued for 30 min at RT. For all preparations, labeling efficiency was determined by instant thin-layer chromatography (ITLC) on TEC Control chromatography strips (Biodex, Shirley, NY). Radiochemical purity of ^{111}In-cetuximab exceeded 97% in all experiments.

Cetuximab was radioiodinated with ^{125}I as described previously.[24] Radiochemical purity of ^{125}I-cetuximab exceeded 99%.

In vitro characteristics of radiolabeled cetuximab

Immunoreactive fraction. The immunoreactive fraction (IRF) of the radiolabeled cetuximab preparations was determined before experiments, using freshly trypsinized FaDu cells as described previously with minor modifications.[25] A serial dilution (3.9×10^4–1.0×10^7 cells/mL) in 0.4 mL RPMI 0.5% BSA was incubated with 200 Bq ^{111}In-cetuximab or ^{125}I-cetuximab in 0.1 mL. Specific activities of ^{111}In-cetuximab and ^{125}I-cetuximab are given in further descriptions of the experiments. A duplicate of the lowest cell concentration was incubated with an excess of unlabeled cetuximab (37.5 μg) to correct for nonspecific binding. After incubation for 20 min at 37°C, cells were washed and the cell-bound activity was determined using a gamma counter (1,480 Wallac Wizard 3", Perkin Elmer, Waltham, MA). The IRF of ^{111}In-cetuximab and ^{125}I-cetuximab used in the experiments exceeded 95%.

Internalization assay. In vitro internalization kinetics of ^{111}In-cetuximab in FaDu cells were determined essentially as described by Koenig *et al.*,[26] with minor modifications. FaDu cells were cultured to confluence in 6-well plates and were incubated with 1,000 Bq ^{111}In-cetuximab (specific activity 0.37 MBq/μg) for 2, 4 or 24 hr in 2 mL binding buffer (RPMI-1640 0.5% BSA), at 37°C in a humidified atmosphere with 5% CO_2. After incubation, cells were washed once with 2 mL ice-cold PBS. One mL of acid wash buffer (0.1 M HAc, 0.15 M NaCl, pH 2.8) was added for 10 min at 37°C to remove the membrane-bound fraction of the cell-associated ^{111}In-cetuximab. Subsequently, cells were washed twice with 1 mL of ice-cold PBS and harvested from the 6-well plates. The amount of membrane-bound and internalized activity was measured in a gamma counter. Nonspecific binding and internalization was determined by coincubation with 5 μg unlabeled cetuximab.

Animal studies

Tumor model. Ninety athymic BALB/*c nu/nu* mice with xenograft FaDu tumors were used in these experiments. Viable 2 mm^3 pieces of FaDu tumor tissue were implanted subcutaneously (s.c.) in the right flank of 6–8 week old mice. Tumors

with a mean diameter of 8 mm were used in the experiments, 2–3 weeks after implantation. Animals were kept in a specific-pathogen-free unit in accordance with institutional guidelines. The Animal Welfare Committee of the Radboud University Nijmegen Medical Centre approved all experiments.

Protein dose escalation study of ^{111}In-cetuximab. For antibody dose escalation study, seven groups of six mice received an intravenous (i.v.) injection in the tail vein of 0.2 MBq ^{111}In-cetuximab (specific activity 0.2 MBq/μg) at increasing protein doses of 1, 3, 10, 30, 100, 300 and 1,000 μg cetuximab per mouse in the respective dose-groups. Mice were euthanized using O_2/CO_2-asphyxiation at 3 days p.i.. Tumors and normal tissues (blood, muscle, lung, liver, spleen, kidney, duodenum and colon) were dissected, weighed and radioactivity uptake was counted in a gamma counter. To correct for radioactive decay, injection standards were counted simultaneously. The activity in counted tissue samples was expressed as percentage of injected dose per gram tissue (%ID/g).

Pharmacodynamics of radiolabeled cetuximab. The pharmacodynamics of ^{111}In-cetuximab and ^{125}I-cetuximab were determined in six groups of six mice. Mice were injected i.v. with 0.2 MBq ^{111}In-cetuximab (specific activity 0.2 MBq/μg) and 0.2 MBq ^{125}I-cetuximab (specific activity 0.2 MBq/μg) with administered total doses cetuximab of either 10 μg (optimal dose) or 3 mg (blocking dose). The blocking dose of unlabeled cetuximab was given to determine non-EGFR-mediated uptake of radiolabeled cetuximab. Mice were euthanized at 1, 3 or 7 days p.i., and uptake of radiolabeled cetuximab was determined as described above.

Autoradiography. Four mice, bearing six s.c. FaDu tumors (unlike in the other experiments, two mice bore a tumor in either flank), were injected i.v. with 2 MBq ^{111}In-cetuximab (total protein dose 10 μg, specific activity 0.36 MBq/μg). Three days after injection, mice were euthanized by cervical dislocation and resected tumors were snap-frozen in liquid nitrogen. Frozen tumors were sectioned using a cryostat microtome. Five-μm tumor sections were mounted on poly-L-lysine coated slides. Selected slides were fixed with cold (4°C) acetone for 10 min, after which they were washed three times using PBS to remove unbound cetuximab. All slides, washed and unwashed, were exposed to a Fujifilm BAS cassette 2,025 overnight (Fuji Photo Film, Tokyo, Japan). Phospholuminescence plates were scanned using a Fuji BAS-1800 II bio-imaging analyzer at a pixel size of 50 × 50 μm. Images were processed with Aida Image Analyzer software (Raytest, Staubenhardt, Germany). The same tumor sections were used for immunohistochemical EGFR staining.

Immunohistochemical staining. Following autoradiography, slides were stained for EGFR expression and blood vessels. Between all consecutive steps of the staining process, sections were rinsed three times for 5 min in 0.1 M PBS, pH 7.4. All primary antibodies were diluted in primary antibody diluent (PAD, Abcam, Cambridge, UK), while secondary antibodies were diluted in PBS. Previously unfixed sections were fixed in cold acetone for 10 min. After rehydration of the tumor sections in PBS for 20 min, they were incubated overnight at 4°C with goat anti-EGFR sc-03 antibody (Santa Cruz Biotechnology, Santa Cruz, CA) diluted 1:100. The EGFR epitope binding sites of sc-03-G (15 amino acids within range 1,000–1,050) and cetuximab (amino acids 310–514) differ,[27] allowing parallel binding of these antibodies to EGFR. Sections were incubated with donkey antigoat Cy3 (Jackson Immunoresearch, West Grove, PA) diluted 1:600 for 30 min at 37°C. This was followed by incubation with 9F1 (rat monoclonal antibody to mouse endothelium, Department of Pathology, Radboud University Nijmegen Medical Centre) undiluted for 45 min at 37°C. Then, sections were incubated with chicken antirat-Alexa647 (Molecular Probes, Leiden, The Netherlands) diluted 1:100 for 60 min at RT. All sections were mounted in Fluorostab (ICN, Zoetermeer, The Netherlands). One adjacent section per tumor was Hematoxylin and Eosin (HE) stained to help distinguish necrotic areas and nontumor tissue from viable tumor areas.

Immunofluorescent image acquisition. The tumor sections were scanned using a digital image processing system consisting of a high-resolution 12-bit CCD camera (Micromax, Roper Scientific, Trenton, NJ) on a fluorescence microscope (Axioskop, Zeiss, Göttingen, Germany) and a computer-controlled motorised stepping stage. Image processing was done using IPLab software (Scanalytics, Fairfax, VA) on a Macintosh computer. Gray scale images (pixel size 2.67 × 2.67 μm) for vessels and EGFR were obtained. Nontumor areas, determined using HE stained neighboring tumor sections, were excluded from analysis.

Colocalization analysis. The autoradiography and immunohistochemistry gray-value images (grayscale range: 256 values) were co-registered using ImageJ Software (JAVA-based image-processing package) and its Turbo-Registration plugin package.[28,29] The pixel size of the immunohistochemistry images was rescaled to match that of the autoradiography images (50 × 50 μm). After alignment, all images were rescaled to a pixel size of 200 × 200 μm, corresponding to the estimated accuracy of image co-registration and compensating for the blurred signal in autoradiograms due to scattering. Prior to rescaling to the 200 × 200-μm pixel size, a mean smoothing of the pixel signal with an appropriate radius was applied to the immunohistochemistry and autoradiography images, to reduce formation of alienating noise artifacts. Matching ROIs were drawn over the aligned tumor sections. Only pixels containing viable tumor tissue were included. The GraphPad Prism 4.0a software package (GraphPad Software, La Jolla, CA) was used to evaluate correlation between the co-registered pixels using the non-parametric Spearman correlation test.

SPECT imaging with ^{111}In-cetuximab. For SPECT imaging, six mice were injected i.v. with 20 MBq ^{111}In-cetuximab

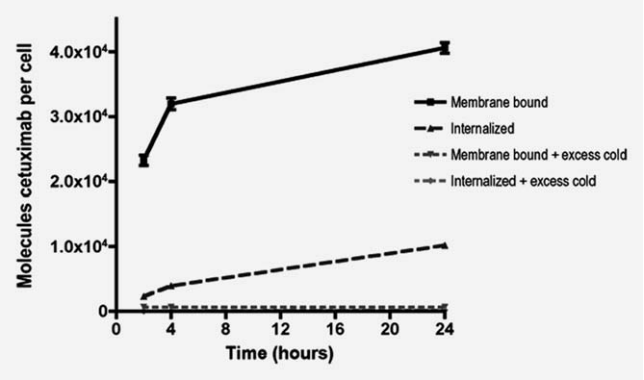

Figure 1. Internalization kinetics of ^{111}In-cetuximab in FaDu cells, with and without addition of excess unlabeled (cold) cetuximab. The number of cetuximab molecules per cell are presented as a function of time. Data are expressed as mean ± SD.

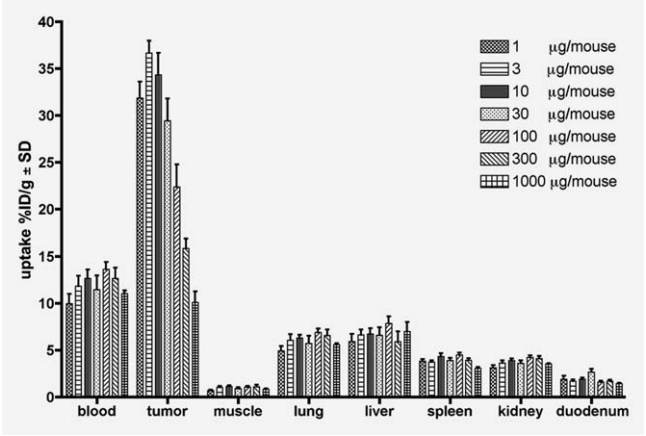

Figure 2. Biodistribution dose escalation study of ^{111}In-cetuximab in mice with subcutaneaously xenografted FaDu tumors, 3 days postinjection. Values are represented as mean %ID/g uptake ± SD for tumors (each bar; $n = 5$) and normal tissues (each bar; $n = 6$). Significant difference was found between uptake of ^{111}In-cetuximab at a protein dose of 100 µg and doses of 1 to 30 µg combined ($p = 0.019$). Comparison of this combined group with 300 µg or 1,000 µg gave highly significant results ($p = 0.0008$). Differences between the 100 µg protein dose-group and the 3 and 10 µg protein dose-groups compared separately were highly significant ($p = 0.0079$).

(total protein dose 10 µg, specific activity 5.55 MBq/µg). SPECT images were acquired directly after injection and 1, 3 and 7 days p.i., using the USPECT II (MILabs, Utrecht, The Netherlands).[30] Mice were scanned in prone position under general anesthesia (isoflurane/N_2O/O_2) for 30–120 min using the 1.0-mm diameter pinhole collimator tube. All mice were euthanized at day 7 and uptake of ^{111}In-cetuximab in dissected tissues was determined as described above. Scans were reconstructed with MILabs reconstruction software, using an ordered-expectation maximization algorithm, with a voxel size of 0.375 mm. Images were analyzed by drawing ROIs over the tumor and the liver region. Tumor-to-liver ratios were determined using mean pixel value thresholded at 40% of maximum pixel value within ROIs with Siemens Inveon Research Workplace software (version 2.2, Siemens Preclinical Solutions, Knoxville, TN).

Statistical analysis

Statistical analyses were performed using Prism software. Differences in uptake of radiolabeled cetuximab were tested for significance using the nonparametric Mann-Whitney test. The nonparametric Spearman test was used to assess correlations between different parameters and a p-value ≤ 0.05 was considered significant.

Results

In vitro internalization of ^{111}In-cetuximab

^{111}In-cetuximab was slowly internalized by FaDu cells (Fig. 1). The fraction ^{111}In-cetuximab that was specifically internalized increased from 3.5% (2.2×10^3 molecules cetuximab per cell) after 2 hr of incubation, to 15.8% (1.0×10^4 molecules cetuximab per cell) after 24 hr. Specifically membrane bound radiolabeled ligand increased from 36.8% (2.3×10^4 molecules cetuximab per cell) after 2 hr incubation, to 64.2% (4.1×10^4 molecules cetuximab per cell) of the added activity after 24 hr.

Protein dose escalation study

A dose escalation study of ^{111}In-cetuximab was performed to determine the optimal cetuximab dose for *in vivo* imaging in the FaDu nude mouse model. ^{111}In-cetuximab showed high specific uptake in FaDu xenograft tumors at cetuximab doses up to 30 µg (mean uptake 33.1 %ID/g ± 3.1) (Fig. 2). At higher doses tumor uptake was significantly lower ($p = 0.019$ to $p = 0.0008$, Fig. 2). Highest antibody-uptake in tumors was observed at protein doses of 10 µg or less (mean uptake 34.3%ID/g ± 2.4; 10 µg: 34.4%ID/g ± 5.2%; 3 µg: 36.7%ID/g ± 2.9 %; 1 µg: 31.9%ID/g ± 3.9%). At the optimal cetuximab doses, tumor-to-blood ratios exceeded 3. Normal mouse tissues, for example liver and lungs, express murine EGFR and cetuximab does not cross-react with these tissues. Assuming that at a cetuximab dose of 1,000 µg per mouse only non-EGFR mediated uptake was measured, this indicated that there was no specific accumulation of ^{111}In-cetuximab in any normal tissue (Fig. 2).

Pharmacodynamics of radiolabeled cetuximab

Tumor uptake of ^{111}In-cetuximab and ^{125}I-cetuximab, at a protein dose of 10 µg per mouse, was highest at 3 days p.i. (Fig. 3). At all time points ^{111}In-cetuximab showed significantly higher uptake in tumors than ^{125}I-cetuximab ($p = 0.002$). Presumably, this is due to internalization of the cetuximab antibody by the FaDu tumor cells, after which the residualizing ^{111}In is retained in the tumor, whereas ^{125}I is mostly excreted from the cells after intracellular degradation

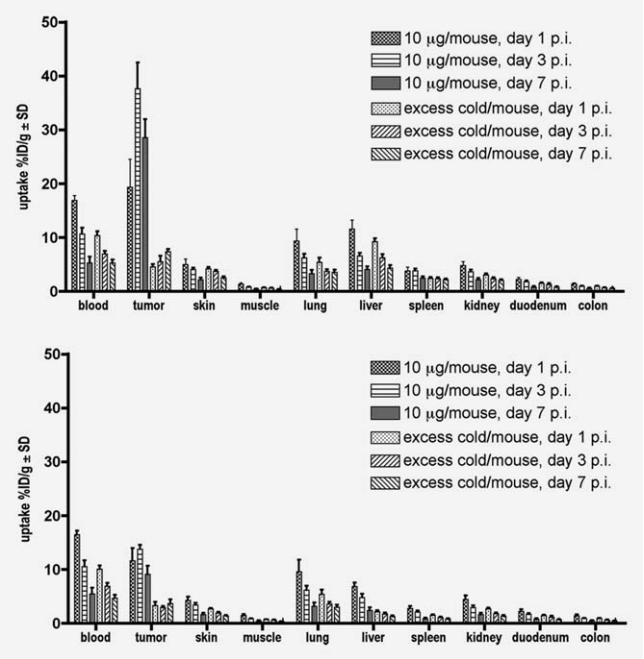

Figure 3. Biodistribution of 10 μg and 3 mg (excess unlabeled) ^{111}In-cetuximab (*a*) and 10 μg and 3 mg (excess unlabeled) ^{125}I-cetuximab (*b*) in mice with subcutaneaously xenografted FaDu tumors 1, 3 and 7 days postinjection. Values are represented as mean %ID/g uptake ± SD for tumors and normal tissues (each bar; $n = 6$).

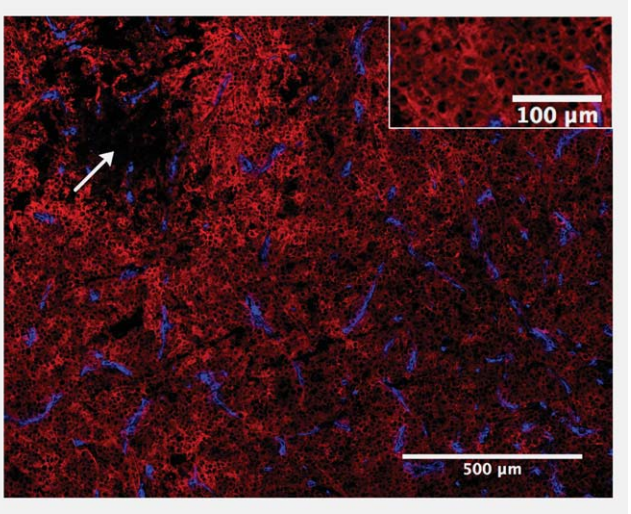

Figure 4. Immunofluorescent image of heterogeneously stained EGFR signal (red) in FaDu tumor located mainly in cell membranes; and vessel staining (blue). Imaging 7 days p.i. of ^{111}In-cetuximab (protein dose 10 μg). White arrow = necrosis. Insert = detail magnification.

of the radiolabeled antibody. Blockage of EGFRs with excess unlabeled cetuximab resulted in a maximum nonspecific uptake of ^{111}In-cetuximab of 7.36 ± 0.98 %ID/g, at 7 days p.i.. Tumor-to-blood ratio of ^{111}In-cetuximab was highest at 7 days p.i. (6.03 ± 1.69 for 10 μg). The highest tumor-to-blood ratio with ^{125}I-cetuximab was also obtained 7 days p.i., but this ratio was much lower (1.91 ± 0.72 for 10 μg).

Immunofluorescent images

Immunohistochemical staining of EGFR in tumor sections dissected after completion of the dose escalation, pharmacodynamic and autoradiography experiments, showed membranous EGFR expression (Fig. 4). EGFR expression was distributed throughout viable tumor tissue, with a heterogeneous intensity staining pattern.

Autoradiography and immunohistochemistry

Autoradiography images of the tumor sections targeted with ^{111}In-cetuximab, and dissected 3 days p.i., showed ^{111}In-cetuximab uptake restricted to viable tumor tissue areas. There were no remarkable differences in uptake pattern or signal intensity between sections that were washed with PBS before autoradiography and unwashed tumor sections. Immunohistochemical staining showed that EGFR distribution was similar to that of ^{111}In-cetuximab uptake patterns on autoradiography (Fig. 5). Pixel-by-pixel analysis of the 8-bit gray value 200 × 200 μm co-registered pixels showed a good correlation between EGFR expression and the localization of ^{111}In-cetuximab in the viable tumor tissue (mean $r = 0.74 \pm 0.14$; range $r = 0.49$–0.86; all correlations $p < 0.0001$).

SPECT imaging

One day p.i., s.c. FaDu tumors were clearly visualized on the USPECT II images (Fig. 6). From that time point onward, tumor uptake stood out distinctly against all other tissues. Tumor-to-liver ratios increased from 0.58 ± 0.24 at day 0 p.i., to 3.42 ± 0.66, 8.99 ± 4.66 and 16.33 ± 11.56 at day 1, day 3 and day 7 p.i., respectively. *Ex vivo* measurements 7 days p.i. showed a mean tumor uptake of ^{111}In-cetuximab of 24.9 ± 15.6 %ID/g. Mean ^{111}In-cetuximab uptake in livers was 2.6 ± 0.7%ID/g. Mean tumor-to-blood ratio was 29.3 ± 20.9 and mean tumor-to-liver ratio 10.6 ± 6.8. Tumor-to-liver ratios calculated from the four immunoSPECT images at 7 days p.i. were a factor ≅1.5 higher than corresponding tumor-to-liver ratios calculated from biodistribution measurements and therefore ratio differences between mice showed a matched trend (6.1 *vs.* 4.1; 8.1 *vs.* 5.0; 20.3 *vs.* 15.4; 30.9 *vs.* 19.9).

Discussion

Our study showed that ^{111}In-cetuximab specifically accumulated in the FaDu head-and-neck xenograft carcinoma model in nude mice, allowing noninvasive imaging of EGFR expression with radiolabeled cetuximab. *In vitro* experiments showed that cetuximab internalized slowly into FaDu tumor cells. ^{111}In-cetuximab showed a higher tumor uptake than ^{125}I-cetuximab at all time points due to the residualizing properties of ^{111}In, which makes it a better suited radionuclide considering the internalizing characteristics of

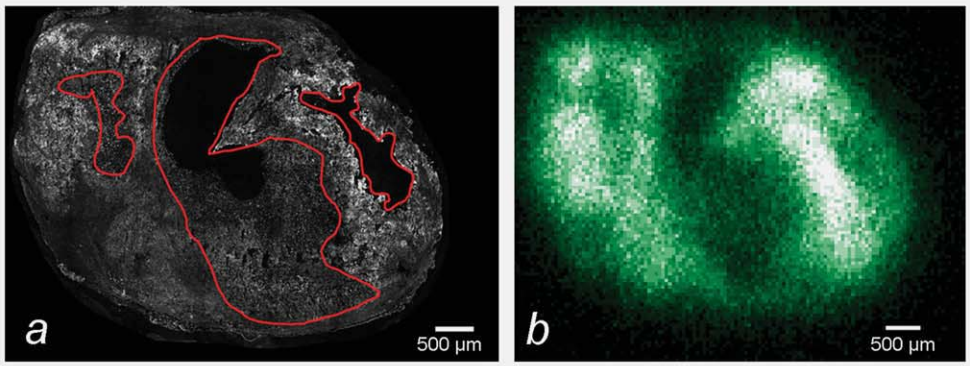

Figure 5. Immunofluorescent gray-value image of EGFR staining (*a*) and autoradiography image of the same tumor section (*b*). Images were made 3 days postinjection of ^{111}In-cetuximab (2 MBq, protein dose 10 µg). In (*a*), red lines enclose nonviable tumor areas, which were excluded from quantification analysis.

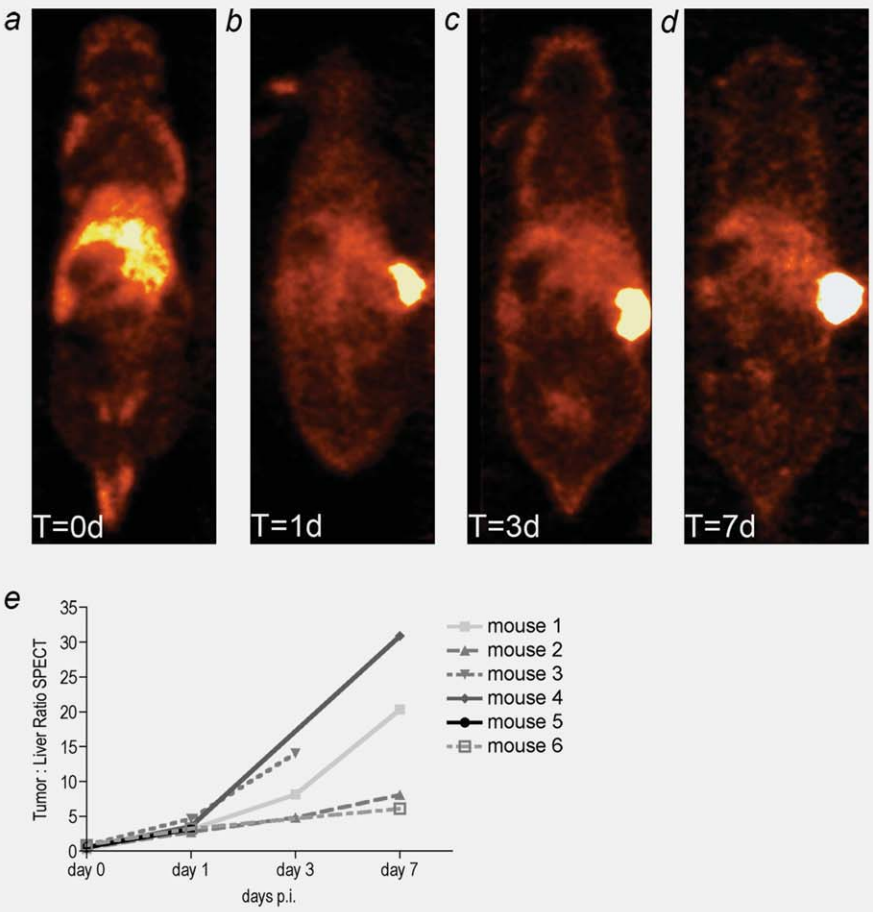

Figure 6. USPECT II images displaying consecutive scans of a mouse with a subcutaneously xenografted FaDu tumor in the right flank. Scanning images directly after injection of ^{111}In-cetuximab (*a*), 1 day (*b*), 3 days (*c*) and 7 days (*d*) p.i. The activity range depicted in each image was corrected for physical and biological decay of ^{111}In-cetuximab. Specific tumor uptake of ^{111}In-cetuximab as registered by USPECT II was compared to nonspecific uptake in the liver as reference background tissue. Tumor-to-liver ratio in imaged animals increased from day 0 until day 7 (*e*).

cetuximab.[31] The dose escalation experiment revealed that ^{111}In-cetuximab displayed the highest uptake in the FaDu tumors at protein doses up to 30 μg per mouse. At higher doses, tumor uptake of ^{111}In-cetuximab in terms of %ID/g decreased, presumably because of saturation of the EGFRs on the cell surface. Also, EGFR downregulation in the tumors may have partially caused this effect. After injection of the determined optimal ^{111}In-cetuximab dose per mouse, FaDu xenograft tumors were clearly visualized with microSPECT. Tumors were the tissue with the highest activity concentration in mice from the imaging time point of 1 day postinjection onwards, and contrast between tumors and other tissues increased until 7 days postinjection. As cetuximab does not cross-react with the murine EGFR, no specific uptake in other tissues, notably the liver, was observed. A good correlation was found between the distribution of ^{111}In-cetuximab and the distribution of EGFR immunohistochemical staining intensity in FaDu tumor sections, indicating that tumor uptake of ^{111}In-cetuximab is a result of its specific interaction with EGFR in all parts of the tumor.

Imaging of EGFR in solid tumors has been subject of investigation for some decades. EGFR expression and tumor uptake properties of radiolabeled cetuximab are well correlated in several preclinical studies,[14,32] but others have not perceived similar results.[13,19] Since utilized radionuclides and administered doses of radiolabeled cetuximab differ between the various reports, as well as tumor models and quantification methods of EGFR expression and tumor uptake of cetuximab, no clear-cut solution to this discrepancy can be presented. Goldenberg *et al.*[33] showed that ^{111}In-labeled murine mAb 225 specifically targeted EGFR overexpressing A431 vulvar squamous cell carcinoma tumors in nude mice. Gamma camera images showed good tumor uptake 3 to 7 days postinjection. Uptake of ^{111}In-labeled mAb 225 was lower in tumors with low EGFR expression (breast cancer models MDA-MB-468 and MCF-7). Dose-dependent receptor blockage was demonstrated in a study performed by Nayak *et al.*,[12] where co-injection of 0.1 or 0.2 mg cetuximab with ^{86}Y-labeled cetuximab resulted in reduced tumor uptake in xenograft tumor models. These findings are in line with our results with ^{111}In-cetuximab: uptake of radiolabeled cetuximab in a nude mice model with xenograft FaDu tumors was optimal at low protein doses. This signifies the importance of using a predetermined model-specific optimal cetuximab dose for imaging. Aerts *et al.*[13] studied uptake of 0.1 mg injected ^{89}Zr-labeled cetuximab in NMRI-*nu* mice with different xenograft tumor types displaying varying EGFR expression levels. In that study, ^{89}Zr-cetuximab uptake did not correlate with EGFR expression levels. This could partly be due to the relatively high protein dose that was used in these models, but the disparity might also be influenced by additional factors. The study suggested that uptake of radiolabeled cetuximab in tumor xenografts is not only determined by EGFR expression levels, but also by other physiological tumor characteristics, like vascular permeability and interstitual fluid pressure. Similarly, Niu *et al.*[18,19] reported that EGFR expression in head-and-neck squamous cell carcinoma xenograft models did not correlate with uptake of ^{64}Cu-labeled panitumumab or ^{64}Cu-DOTA-cetuximab and that vascular density and permeability of the tumor models probably influenced compound accumulation. In our studies of the FaDu tumor model, autoradiograpic analysis showed ^{111}In-cetuximab uptake signal dispersed throughout viable tumor tissue and good correlation with EGFR signal intensity patterns, suggesting that EGFR expression was an important factor determining ^{111}In-cetuximab uptake.

When translating preclinical imaging results to the clinical situation, behavior of radiolabeled antibodies as well as physical research model traits should be taken into account. Radionuclides used for imaging should be adjusted to the inherent properties of studied antibodies. Radionuclides with a short physical half-life, such as ^{64}Cu (12 hr) or ^{99m}Tc (6 hr), might not be appropriate because of incompatibility with the slow pharmacokinetics and clearance of cetuximab (in humans T1/2 $\cong$ 112 hr). Imaging of EGFR expression in tumors will probably not be feasible during cetuximab-based therapy, because therapeutic doses of cetuximab will block the target antigen in the tumor. Therefore, radiolabeled cetuximab might best be applied to select patients applicable for cetuximab therapy, and to assess response at later time points during follow-up. EGFR imaging with radiolabeled cetuximab could however be applied in early response evaluation of modalities such as radiotherapy or therapies involving tyrosine kinase inhibitors. Due to the slow pharmacokinetics of radiolabeled cetuximab, an interval of 1–7 days between administration and (SPECT) imaging would be used. It would be logistically attractive to evaluate accumulation of a radiotracer in tumors within 1 day after administration. Radiolabeled antibody fragments, tyrosine kinase inhibitors and the natural ligand EGF are candidates for fast imaging of tumor EGFR expression. Due to their low molecular weights, these tracers permeate rapidly into the target tissue and display fast background clearance. However, previous studies have shown that these agents generally have much lower uptake in the target tissue than intact IgG antibodies.[34–38]

Naturally occurring mutations of the EGFR-gene have been described, of which a truncation mutation, EGFR variant III (EGFRvIII), is expressed in up to 42% of head-and-neck squamous cell carcinomas.[39] Since cetuximab also binds to, and downregulates, EGFRvIII,[40] imaging of EGFRwildtype as well as EGFRvIII with radiolabeled cetuximab is also relevant in tumors exhibiting this truncated dominant-active variant.[41]

The liver displays relatively high levels of EGFR.[38] Hepatic sequestration of radiolabeled cetuximab might impede reliable visualization of tumor EGFR expression.[20,21,42] The presence of such an antigen sink might require administration of higher doses of radiolabeled cetuximab for tumor imaging in patients. Divgi *et al.*[20] reported that uptake of ^{111}In-labeled mAb 225

in squamous cell carcinoma of the lung was dose-dependent in patients and that up to 40 mg of cetuximab would be captured by the liver before any tumors could be discerned on imaging. This particular phenomenon cannot be studied in preclinical mouse-xenograft models, since cetuximab does not cross-react with the murine EGFR. The accretion of radiolabeled cetuximab in the liver in mice is due to nonspecific mechanisms.[16] Studies with antibodies cross-reactive with murine EGFR would be needed to study the effect of EGFR expression in the liver in a mouse model.

Tumor-to-liver uptake ratio of EGFR imaging tracers might be improved by preadministration of unlabeled blocking agents as was shown in a mouse-xenograft model,[38] although the timing and appropriate dose might be difficult to determine in patients.[21]

Nevertheless, defining the appropriate radiolabeled cetuximab dose for optimal imaging outcomes in head-and-neck cancer patients is a prerequisite. These and other matters, such as appropriate timing of imaging after injection and specification of the imaging purpose (*e.g.*, treatment selection or therapy response evaluation) should be considered before introducing radiolabeled cetuximab into clinical practice as an attribution to the diagnostic armamentarium of head-and-neck cancer.

Conclusion

Optimally dosed ^{111}In-cetuximab accumulated efficiently in FaDu head-and-neck squamous cell carcinoma xenografts. Tumors could be visualized from one day postinjection onward using SPECT and tumor-to-background contrast increased with time. ^{111}In-cetuximab accumulation in tumor sections correlated well with immunohistochemical distribution of EGFR, suggesting that imaging uptake reflected actual tumor EGFR expression.

Acknowledgements

We thank Sandra Heskamp, Bianca Lemmers-van de Weem, Kitty Lemmens-Hermans, Hans Peters and Jasper Lok for technical assistance.

References

1. Herbst RS. Review of epidermal growth factor receptor biology. *Int J Radiat Oncol Biol Phys* 2004;59:21–6.
2. Bussink J, Kaanders JH, van der Kogel AJ. Microenvironmental transformations by VEGF- and EGF-receptor inhibition and potential implications for responsiveness to radiotherapy. *Radiother Oncol* 2007;82:10–7.
3. Bussink J, van der Kogel AJ, Kaanders JH. Activation of the PI3-K/AKT pathway and implications for radioresistance mechanisms in head and neck cancer. *Lancet Oncol* 2008;9:288–96.
4. Nicholson RI, Gee JM, Harper ME. EGFR and cancer prognosis. *Eur J Cancer* 2001; 37(Suppl 4):S9–15.
5. Ang KK, Berkey BA, Tu X, Zhang HZ, Katz R, Hammond EH, Fu KK, Milas L. Impact of epidermal growth factor receptor expression on survival and pattern of relapse in patients with advanced head and neck carcinoma. *Cancer Res* 2002;62: 7350–6.
6. Sunada H, Magun BE, Mendelsohn J, MacLeod CL. Monoclonal antibody against epidermal growth factor receptor is internalized without stimulating receptor phosphorylation. *Proc Natl Acad Sci USA* 1986;83:3825–9.
7. Meyerhardt JA, Mayer RJ. Systemic therapy for colorectal cancer. *N Engl J Med* 2005;352:476–87.
8. Vermorken JB, Mesia R, Rivera F, Remenar E, Kawecki A, Rottey S, Erfan J, Zabolotnyy D, Kienzer HR, Cupissol D, Peyrade F, Benasso M, et al. Platinum-based chemotherapy plus cetuximab in head and neck cancer. *N Engl J Med* 2008; 359:1116–27.
9. Bonner JA, Harari PM, Giralt J, Azarnia N, Shin DM, Cohen RB, Jones CU, Sur R, Raben D, Jassem J, Ove R, Kies MS, et al. Radiotherapy plus cetuximab for squamous-cell carcinoma of the head and neck. *N Engl J Med* 2006;354:567–78.
10. Bonner JA, Harari PM, Giralt J, Cohen RB, Jones CU, Sur RK, Raben D, Baselga J, Spencer SA, Zhu J, Youssoufian H, Rowinsky EK, et al. Radiotherapy plus cetuximab for locoregionally advanced head and neck cancer: 5-year survival data from a phase 3 randomised trial, and relation between cetuximab-induced rash and survival. *Lancet Oncol* 2010;11:21–8.
11. Bussink J, van Herpen CM, Kaanders JH, Oyen WJ. PET-CT for response assessment and treatment adaptation in head and neck cancer. *Lancet Oncol* 2010;11:661–9.
12. Nayak TK, Regino CA, Wong KJ, Milenic DE, Garmestani K, Baidoo KE, Szajek LP, Brechbiel MW. PET imaging of HER1-expressing xenografts in mice with 86Y-CHX-A"-DTPA-cetuximab. *Eur J Nucl Med Mol Imaging* 2010;37:1368–76.
13. Aerts HJ, Dubois L, Perk L, Vermaelen P, van Dongen GA, Wouters BG, Lambin P. Disparity Between In Vivo EGFR Expression and 89Zr-Labeled Cetuximab Uptake Assessed with PET. *J Nucl Med* 2009;50:123–31.
14. Cai W, Chen K, He L, Cao Q, Koong A, Chen X. Quantitative PET of EGFR expression in xenograft-bearing mice using 64Cu-labeled cetuximab, a chimeric anti-EGFR monoclonal antibody. *Eur J Nucl Med Mol Imaging* 2007;34:850–8.
15. Ping Li W, Meyer LA, Capretto DA, Sherman CD, Anderson CJ. Receptor-binding, biodistribution, and metabolism studies of 64Cu-DOTA-cetuximab, a PET-imaging agent for epidermal growth-factor receptor-positive tumors. *Cancer Biother Radiopharm* 2008;23:158–71.
16. Milenic DE, Wong KJ, Baidoo KE, Ray GL, Garmestani K, Williams M, Brechbiel MW. Cetuximab: preclinical evaluation of a monoclonal antibody targeting EGFR for radioimmunodiagnostic and radioimmunotherapeutic applications. *Cancer Biother Radiopharm* 2008;23: 619–31.
17. Barrett T, Koyama Y, Hama Y, Ravizzini G, Shin IS, Jang BS, Paik CH, Urano Y, Choyke PL, Kobayashi H. In vivo diagnosis of epidermal growth factor receptor expression using molecular imaging with a cocktail of optically labeled monoclonal antibodies. *Clin Cancer Res* 2007;13: 6639–48.
18. Niu G, Li Z, Xie J, Le QT, Chen X. PET of EGFR antibody distribution in head and neck squamous cell carcinoma models. *J Nucl Med* 2009;50:1116–23.
19. Niu G, Sun X, Cao Q, Courter D, Koong A, Le QT, Gambhir SS, Chen X. Cetuximab-based immunotherapy and radioimmunotherapy of head and neck squamous cell carcinoma. *Clin Cancer Res* 2010;16:2095–105.
20. Divgi CR, Welt S, Kris M, Real FX, Yeh SD, Gralla R, Merchant B, Schweighart S, Unger M, Larson SM, Mendelsohn J. Phase I and imaging trial of indium 111-labeled anti-epidermal growth factor receptor monoclonal antibody 225 in patients with squamous cell lung carcinoma. *J Natl Cancer Inst* 1991;83:97–104.

21. Schechter NR, Wendt RE, III, Yang DJ, Azhdarinia A, Erwin WD, Stachowiak AM, Broemeling LD, Kim EE, Cox JD, Podoloff DA, Ang KK. Radiation dosimetry of 99mTc-labeled C225 in patients with squamous cell carcinoma of the head and neck. *J Nucl Med* 2004;45:1683–7.
22. Naramura M, Gillies SD, Mendelsohn J, Reisfeld RA, Mueller BM. Therapeutic potential of chimeric and murine anti-(epidermal growth factor receptor) antibodies in a metastasis model for human melanoma. *Cancer Immunol Immunother* 1993;37:343–9.
23. Goldstein NI, Prewett M, Zuklys K, Rockwell P, Mendelsohn J. Biological efficacy of a chimeric antibody to the epidermal growth factor receptor in a human tumor xenograft model. *Clin Cancer Res* 1995;1:1311–8.
24. Heskamp S, van Laarhoven HW, Molkenboer-Kuenen JD, Versleijen-Jonkers YM, Oyen WJ, van der Graaf WT, Boerman OC. ImmunoSPECT and immunoPET imaging of IGF-1R expression with radiolabeled R1507 in a triple negative breast cancer model. *J Nucl Med* 2010;51:1565–72.
25. Lindmo T, Boven E, Cuttitta F, Fedorko J, Bunn PA, Jr. Determination of the immunoreactive fraction of radiolabeled monoclonal antibodies by linear extrapolation to binding at infinite antigen excess. *J Immunol Methods* 1984;72:77–89.
26. Koenig JA, Kaur R, Dodgeon I, Edwardson JM, Humphrey PP. Fates of endocytosed somatostatin sst2 receptors and associated agonists. *Biochem J* 1998;336(Pt 2):291–8.
27. Li S, Schmitz KR, Jeffrey PD, Wiltzius JJ, Kussie P, Ferguson KM. Structural basis for inhibition of the epidermal growth factor receptor by cetuximab. *Cancer Cell* 2005;7:301–11.
28. Thevenaz P, Ruttimann UE, Unser M. A pyramid approach to subpixel registration based on intensity. *IEEE Trans Image Process* 1998;7:27–41.
29. Hoeben BA, Kaanders JH, Franssen GM, Troost EG, Rijken PF, Oosterwijk E, van Dongen GA, Oyen WJ, Boerman OC, Bussink J. PET of Hypoxia with 89Zr-Labeled cG250-F(ab')2 in Head and Neck Tumors. *J Nucl Med* 2010;51:1076–83.
30. van der Have F, Vastenhouw B, Ramakers RM, Branderhorst W, Krah JO, Ji C, Staelens SG, Beekman FJ. U-SPECT-II: An ultra-high-resolution device for molecular small-animal imaging. *J Nucl Med* 2009;50:599–605.
31. Brouwers AH, Buijs WC, Oosterwijk E, Boerman OC, Mala C, de Mulder PH, Corstens FH, Mulders PF, Oyen WJ. Targeting of metastatic renal cell carcinoma with the chimeric monoclonal antibody G250 labeled with (131)I or (111)In: an intrapatient comparison. *Clin Cancer Res* 2003;9:3953S–60S.
32. Eiblmaier M, Meyer LA, Watson MA, Fracasso PM, Pike LJ, Anderson CJ. Correlating EGFR expression with receptor-binding properties and internalization of 64Cu-DOTA-cetuximab in 5 cervical cancer cell lines. *J Nucl Med* 2008;49:1472–9.
33. Goldenberg A, Masui H, Divgi C, Kamrath H, Pentlow K, Mendelsohn J. Imaging of human tumor xenografts with an indium-111-labeled anti-epidermal growth factor receptor monoclonal antibody. *J Natl Cancer Inst* 1989;81:1616–25.
34. Brouwers A, Mulders P, Oosterwijk E, Buijs W, Corstens F, Oyen W, Boerman C. Pharmacokinetics and tumor targeting of 131I-labeled F(ab')2 fragments of the chimeric monoclonal antibody G250: preclinical and clinical pilot studies. *Cancer Biother Radiopharm* 2004;19:466–77.
35. Nordberg E, Orlova A, Friedman M, Tolmachev V, Stahl S, Nilsson FY, Glimelius B, Carlsson J. In vivo and in vitro uptake of 111In, delivered with the affibody molecule (ZEGFR:955)2, in EGFR-expressing tumour cells. *Oncol Rep* 2008;19:853–7.
36. Pantaleo MA, Nannini M, Maleddu A, Fanti S, Nanni C, Boschi S, Lodi F, Nicoletti G, Landuzzi L, Lollini PL, Biasco G. Experimental results and related clinical implications of PET detection of epidermal growth factor receptor (EGFr) in cancer. *Ann Oncol* 2009;20:213–26.
37. Xu N, Cai G, Ye W, Wang X, Li Y, Zhao P, Zhang A, Zhang R, Cao B. Molecular imaging application of radioiodinated anti-EGFR human Fab to EGFR-overexpressing tumor xenografts. *Anticancer Res* 2009;29:4005–11.
38. Kareem H, Sandstrom K, Elia R, Gedda L, Anniko M, Lundqvist H, Nestor M. Blocking EGFR in the liver improves the tumor-to-liver uptake ratio of radiolabeled EGF. *Tumor Biol* 2010;31:79–87.
39. Sok JC, Coppelli FM, Thomas SM, Lango MN, Xi S, Hunt JL, Freilino ML, Graner MW, Wikstrand CJ, Bigner DD, Gooding WE, Furnari FB, et al. Mutant epidermal growth factor receptor (EGFRvIII) contributes to head and neck cancer growth and resistance to EGFR targeting. *Clin Cancer Res* 2006;12:5064–73.
40. Patel D, Lahiji A, Patel S, Franklin M, Jimenez X, Hicklin DJ, Kang X. Monoclonal antibody cetuximab binds to and down-regulates constitutively activated epidermal growth factor receptor vIII on the cell surface. *Anticancer Res* 2007;27:3355–66.
41. Aerts HJ, Dubois L, Hackeng TM, Straathof R, Chiu RK, Lieuwes NG, Jutten B, Weppler SA, Lammering G, Wouters BG, Lambin P. Development and evaluation of a cetuximab-based imaging probe to target EGFR and EGFRvIII. *Radiother Oncol* 2007;83:326–32.
42. Vallis KA, Reilly RM, Chen P, Oza A, Hendler A, Cameron R, Hershkop M, Iznaga-Escobar N, Ramos-Suzarte M, Keane P. A phase I study of 99mTc-hR3 (DiaCIM), a humanized immunoconjugate directed towards the epidermal growth factor receptor. *Nucl Med Commun* 2002;23:1155–64.